Since January 2020 Elsevier has created a COVID-19 resource centre with free information in English and Mandarin on the novel coronavirus COVID-19. The COVID-19 resource centre is hosted on Elsevier Connect, the company's public news and information website.

Journal Pre-proof

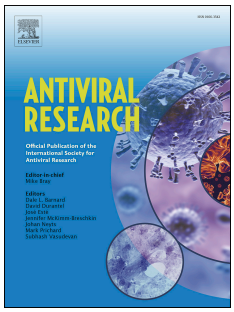

Cathepsin inhibitors nitroxoline and its derivatives inhibit SARS-CoV-2 infection

Rafaela Milan Bonotto, Ana Mitrović, Izidor Sosič, Pamela Martinez-Orellana, Federica Dattola, Stanislav Gobec, Janko Kos, Alessandro Marcello

PII: S0166-3542(23)00133-X

DOI: https://doi.org/10.1016/j.antiviral.2023.105655

Reference: AVR 105655

To appear in: *Antiviral Research*

Received Date: 26 January 2023

Revised Date: 13 June 2023

Accepted Date: 14 June 2023

Please cite this article as: Milan Bonotto, R., Mitrović, A., Sosič, I., Martinez-Orellana, P., Dattola, F., Gobec, S., Kos, J., Marcello, A., Cathepsin inhibitors nitroxoline and its derivatives inhibit SARS-CoV-2 infection, *Antiviral Research* (2023), doi: https://doi.org/10.1016/j.antiviral.2023.105655.

Cathepsin inhibitors Nitroxoline and its derivatives inhibit SARS-CoV-2 infection

*Rafaela Milan Bonotto[1], *Ana Mitrović[2,3], Izidor Sosič[3], Pamela Martinez-Orellana[1], Federica Dattola[1], Stanislav Gobec[3], Janko Kos[2,3] and Alessandro Marcello[1]

*Contributed equally to this work

[1]Laboratory of Molecular Virology, The International Centre for Genetic Engineering and Biotechnology (ICGEB), Padriciano, 99, 34149 Trieste, Italy.
[2]Department of Biotechnology, Jožef Stefan Institute, Jamova 39, 1000 Ljubljana, Slovenia
[3]Faculty of Pharmacy, University of Ljubljana, Aškerčeva cesta 7, 1000 Ljubljana, Slovenia

Corresponding authors:
Janko Kos
Faculty of Pharmacy
University of Ljubljana
Aškerčeva cesta 7, 1000 Ljubljana, Slovenia
Email: janko.kos@ffa.uni-lj.si
www.ffa.uni-lj.si

Alessandro Marcello, PhD
Laboratory of Molecular Virology
International Centre for Genetic Engineering and Biotechnology (ICGEB)
Padriciano, 99, 34149 Trieste, Italy
Email: marcello@icgeb.org
www.icgeb.org/molecular-virology.html

Abstract

The severity of the SARS-CoV-2 pandemic and the recurring (re)emergence of viruses prompted the development of new therapeutic approaches that target viral and host factors crucial for viral infection. Among them, host peptidases cathepsins B and L have been described as essential enzymes during SARS-CoV-2 entry. In this study, we evaluated the effect of potent selective cathepsin inhibitors as antiviral agents. We demonstrated that selective cathepsin B inhibitors, such as the antimicrobial agent nitroxoline and its derivatives, impair SARS-CoV-2 infection *in vitro*. Antiviral activity observed at early stage of virus entry was cell-type dependent and correlated well with the intracellular content and enzymatic function of cathepsins B or L. Furthermore, tested inhibitors were effective against the ancestral SARS-CoV-2 D614 as well as against the more recent BA.1_4 (Omicron). Taken together, our results highlight the important role of host cysteine cathepsin B in SARS-CoV-2 virus entry and show that cathepsin-specific inhibitors, such as nitroxoline and its derivatives, could be used to treat COVID-19. Finally, these results also suggest that nitroxoline has potential to be further explored as repurposed drug in antiviral therapy.

Highlights:

- Cathepsins are key host factors for SARS-CoV-2 entry.
- Cathepsin B inhibitors are active against SARS-CoV-2.
- Cathepsin activity is cell-type dependent.
- The antibiotic nitroxoline is a candidate for drug repurposing.

Keywords:

SARS-CoV-2, COVID-19, Coronavirus, Cathepsin, Nitroxoline, Drug repurposing, Inhibition

1. Introduction

Severe Acute Respiratory Syndrome Coronavirus 2 (SARS-CoV-2) is the aetiologic agent of Coronavirus Disease (COVID-19). Since its first appearance at the end of 2019, several successive waves of infections have had a tremendous impact on the lives of millions of people worldwide, causing the most severe pandemics in recent history (CoVariants, 2022; 2021). Notwithstanding, the availability of effective vaccines and monoclonal antibodies, the ongoing evolution of the virus continuously works to evade the immune response. Specific antiviral drugs have been developed, such as the clinically approved molnupiravir and remdesivir, which target the viral polymerase, and the paxlovid, which targets viral proteases (Gottlieb et al., 2022; Jayk Bernal et al., 2022; Kokic et al., 2021; Marzi et al., 2022). However, continued efforts are needed to increase the availability of broad-spectrum antivirals that can act against different virus strains for future emerging or re-emerging epidemics (Dolgin, 2021; Liu et al., 2020; Zakaria et al., 2018).

Host cell peptidases are critical in various steps of virion entry into host cells (Pišlar et al., 2020). Entry of SARS-CoV-2 occurs by binding of the Spike (S) protein to the cellular receptor angiotensin converting enzyme 2 (ACE2) and activation for membrane fusion by the transmembrane peptidase/serine subfamily member 2 (TMPRSS2), or by other transmembrane serine peptidases at the cell surface. Alternatively, the virus enters by receptor-mediated endocytosis, in which host endosomal/lysosomal cysteine peptidases, such as cathepsins B (CatB) and L (CatL), are involved in S protein activation (Evans and Liu, 2021; Pišlar et al., 2020; Shang et al., 2020). The main function of CatL and CatB is intracellular protein catabolism in endosomal/lysosomal compartments (Turk et al., 2000). However, a number of more specific functions have been identified, often associated with pathological processes, including cancer, neurodegeneration, and viral infections (Simmons et al., 2013). The involvement of cysteine cathepsins in virion entry has been previously described for several other non-enveloped and enveloped viruses (Evans and Liu, 2021; Pišlar et al., 2020; Shang et al., 2020) and confirmed also for SARS-CoV-2 (Hoffmann et al., 2020).

Among host cysteine peptidases, CatL is the most commonly associated with viral glycoprotein activation due to its ability to process the SARS-CoV-2 S protein and related proteins of other human CoVs (Gomes et al., 2020; Kawase et al., 2009; Liu et al., 2020; Shirato et al., 2013; Simmons et al., 2005). CatL has been identified as an essential lysosomal peptidase for virion entry into cells stably expressing recombinant human ACE2 (Ou et al., 2020). CatB has been shown to play a role in Ebola virus (Chandran et al., 2005), Nipah virus (Diederich et al., 2008),

and feline CoV (Regan et al., 2008) entry through catalytic activation of viral membrane glycoproteins.

Investigation of the role of CatB and CatL in various pathologies resulted in development of a large number of inhibitors (Dana and Pathak, 2020; Kos et al., 2014). We evaluated the well-established antimicrobial agent nitroxoline, identified by our group as a potent selective inhibitor of CatB (Mirković et al., 2015; Mirković et al., 2011), for its activity against SARS-CoV-2. In this study, we show that nitroxoline and its derivatives, which are specific for CatB, potently prevent SARS-CoV-2 entry into the host cells. Antiviral activity was dependent on cell type and correlated well with the intracellular amount and activity of the targeted cathepsin. Thus, we demonstrate the critical role of the host CatB in SARS-CoV-2 infection and suggest that nitroxoline can be repurposed as potential therapeutic agents for clinical intervention against SARS-CoV-2.

2. Materials and methods

2.1 Cells and virus

Vero E6 cells (ATCC-1586), Huh7 cells expressing hACE2 (Huh7-hACE2) (Milani et al. 2021), and human lung adenocarcinoma cells Calu-3 (ATCC HTB-55) were cultured in Dulbecco's modified Eagle's medium (DMEM, ThermoFisher, Paisley, UK) supplemented with 10% foetal bovine serum (FBS, ThermoFisher, Paisley, UK). All cell lines were obtained from the American Type Culture Collection (ATCC). Human Nasal Epithelial cells (HNEpC), PromoCell cat number c-12620, were grown in Airway Epithelial cell Growth Medium (ready-to-use) PromoCell cat number C-21060. The same protocol was used for Human Pulmonary Alveolar Epithelial Cells (HPAEpC) Catalog #3200 ScienCell Research Laboratories growing in complete PneumaCult-ALI-S cat number #05051 Stemcell technologies.

Working strains of SARS-CoV-2 ICGEB-FVG_5 (Licastro et al., 2020) (ancestral strain with D614G mutation) and the Omicron variant SARS-CoV-2 BA.1_4 isolated in Trieste, Italy, were routinely propagated and titrated as described elsewhere (Milani et al., 2021).

2.2 Inhibitors

Hydroxychloroquine, nitroxoline, E-64 and E-64d were purchased from Sigma-Aldrich (St. Luis, USA). Nitroxoline derivatives compounds **3** (Mirković et al., 2011) and **17** (Sosič et al., 2013) were synthesised as reported. Their purity was determined by ^{1}H NMR and ^{13}C NMR spectroscopy and by CHN elemental analysis and tested for specificity against other cysteine cathepsins (Mirković et al., 2011; Sosič et al., 2013). CLIK-148 was kindly provided by prof. Nobuhiko Katunuma (The University of Tokushima, Tokushima, Japan). Compound GCV-5 (Mitrović et al., 2022) was obtained from MolPort (Riga, Latvia). The structures are shown in Figure S1. The compounds were dissolved in DMSO, expect for hydroxychloroquine (HCQ), which was prepared in water, and stored at -20 °C until use. Physicochemical properties of compounds **3** and **17**, such as efflux ratio, albumin binding, logP and solubility were determined using QikProp (Schrödinger Suite 2020–2, Schrödinger, LLC, New York, NY, 2020) and are presented in the Supplementary Information .

2.3 High content assay (HCA)

Drugs were tested for antiviral activity with a previously optimized protocol on Huh7 cells expressing hACE2 (Milani et al., 2021). briefly, cells were treated and simultaneously infected with virus for 24 hours on 96-wells plates and processed for immunofluorescence with antibodies against SARS-CoV-2 Spike or Nucleocapsid. Images were automatically acquired,

and the total number of cells and the number of infected cells were analysed by hogh-contnt imaging. Extended protocols are available in Supplementary Methods.

2.4 Virological methods

Vero E6 cells were used for plaque assay using 1.5% carboxymethylcellulose (CMC, Sigma-Aldrich, St Louis, USA) as previously described (Rajasekharan et al., 2021) . To calculate viral yields, infected cells' medium was collected after 24 h and the viral titre for each concentration was determined by the plaque assay. Viability assay was performed using the Alamar Blue reagent according to manufacturer specifications (Invitrogen, Waltham, MA, USA). Time of addition studies (TOA) were performed on infected Huh7-hACE2 as described (Milan Bonotto et al., 2022). Briefly, drugs were added 3 hours before infection, or during infection, and washed away or added after 1, 3, 5 hours post-infection and in all cases kept until harvest after 24 h. Binding of the virus to cells was conducted at 4 °C for two hours in the presence of the drug as described (Milan Bonotto et al., 2022). To measure entry cells were washed after the binding step and further incubate at 37 °C for 3 h before harvest. Extended protocols are available in Supplementary Methods.

2.5 Protein preparation, Western blot analysis and ELISA

Cells were detached from culture flasks, lysed, and processed for Western blotting as previously described (Mitrović et al., 2016). ELISA was performed as previously described (Kos et al., 2005). Extended protocols are available in Supplementary Methods.

2.6 Determination of cathepsin activity

CatB activity was measured using specific fluorogenic substrates as described in detail in extended protocols available in Supplementary Methods.

2.7 Statistical analysis

The sigmoidal dose-response curve function (variable slope) was used to calculate the half maximal effective (EC_{50}) and cytotoxic (CC_{50}) concentrations was calculated using GraphPad Prism version 7 (GraphPad Software, San Diego, USA). The ratio between CC_{50} and EC_{50} determines the selective index (SI). To calculate the statistical significance ($P < 0.05$) of infected and DMSO treated samples a two-way analysis of variance (ANOVA) with Sidak's test, a multiple comparison test, was conducted. All data were plotted and analysed using GraphPad Prism software version 7.

Results

3.1 Screening of a panel of cathepsin inhibitors against SARS-CoV-2

Screening of cathepsin inhibitors was performed using a previously developed High Content assay (HCA) (Milani et al., 2021). The control hydroxychloroquine (HCQ) was active with an inhibitory concentration EC_{50} of 4.75 ± 0.35 μM. Nitroxoline and compound **17** inhibited more than 90% of SARS-CoV-2 infection at the highest concentration tested (100 μM) with an EC_{50} of 2 ± 0.003 μM and 2.8 ± 0.048 μM, respectively (Table 1, Figure 1). Compound **3**, that inhibits both CatB and CatL (our unpublished data), showed a higher EC_{50} value (4.5 ± 2.1 μM). Surprisingly, the general cathepsin epoxy-succinyl irreversible inhibitor E-64 inhibited the virus only at high concentrations (> 70 μM), whereas its cell-permeable analogue E-64d showed EC_{50} = 1.9 ± 0.10 μM (Table 1). However, neither E-64 nor E-64d reached >90% inhibition (Figure S2). Compound CLIK-148, a specific CatL inhibitor, provided EC_{50} value of 8.75 ± 6.2 μM and reached a maximum of 64% antiviral activity at the highest concentration tested. In contrast, GCV-5, another CatL inhibitor, failed to provide EC_{50} values and showed no antiviral activity against SARS-CoV-2. All compounds were not toxic to cells under conditions tested, except for GCV-5. These results demonstrate that CatB inhibitors are most potent against SARS-CoV-2 in Huh7-hACE2 cells.

Table 1. Dose-response results from cathepsin inhibitors in Huh7-hACE2 infected with SARS-CoV2 D614G

	EC_{50} [a] **µM (mean± SD [b])**	EC_{90} [c] **µM (mean± SD)**	CC_{50} [d] **µM**	**Highest % of Virus Inhibition**
Nitroxoline	2.1±0.003	9.9± 8	>100	99
Compound 17	2.8±0.04	6.4± 0.3	>100	98
Compound 03	4.5±2.1	11.9± 0.9	>100	80
E64	73 ±8.3	n.a	> 100	61
E64-d	1.9±0.10	n.a	> 100	79
CLIK 148	8.75± 6.2	n.a	>100	64
GCV-5	n.a*	n.a*	n.a*	n.a*
Hydroxychloroquin[e]	4.7± 0.35	18.9± 2.3	>100	98

*n.a not assessable

[a] Half maximal effective concentration from values obtained in HCA

[b] Standard deviation

[c] Maximal effective concentration from values obtain in HCA

[d] Half maximal cytotoxic concentration from values obtained in HCA

[e] Reference compound, positive control

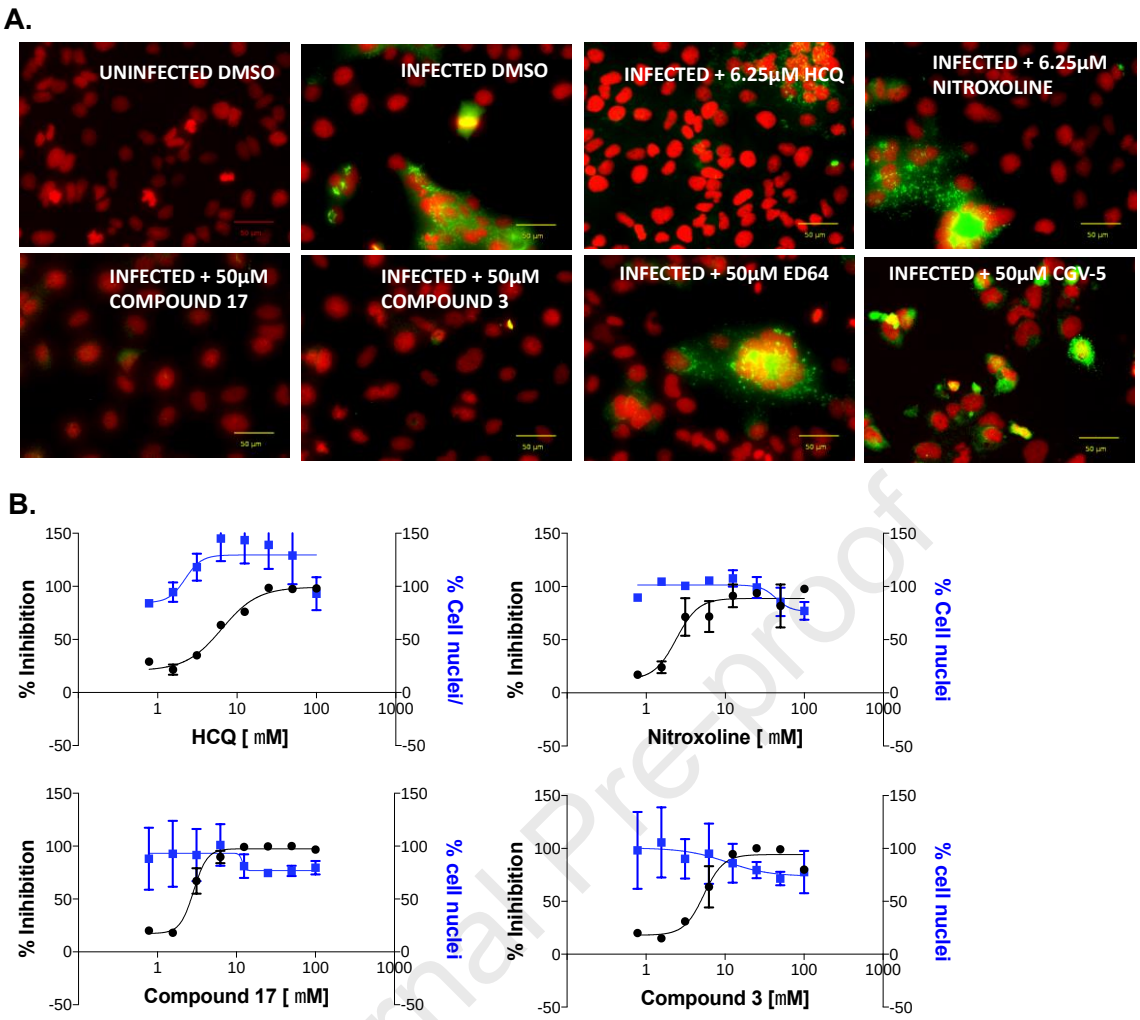

Figure 1. Nitroxoline, compound 17 and compound 3 efficiently inhibit SARS-CoV2 D614G infection in Huh7-hACE2 cells.

(**A**) Representative images from High Content assay (HCA) showing infection of SARS-CoV-2 D614G in Huh7-hACE2 at 24 hpi. Cells were infected and treated with the inhibitors simultaneously for 24 h. Then cells were fixed and processed for immunofluorescence with the anti-nucleocapsid antibody (green fluorescence). Nuclei were stained with DAPI (red fluorescence).

(**B**) Huh7-hACE2 were treated with 2-fold dilutions of compound and simultaneously infected with SARS-CoV-2 D614G at MOI 0.1. Hydroxychloroquine (HCQ) was used as the reference compound (positive control). Cells were processed for high-content image analysis as described. The percentage of inhibition (black dots) was normalized by the average infection ratio of cells treated with 1% DMSO (vehicle). The percentage of nuclei (blue triangles) was normalized with the total number of cells.

3.2 Cathepsin inhibitors show cell-dependent activity against SARS-CoV-2

Cathepsins are host peptidases and their expression and activity varies depending on the cell type (Yadati et al., 2020). SARS-CoV-2 replicates efficiently in lung- and kidney-derived cells, such as human adenocarcinoma Calu-3 cells and Vero E6 cells (Cagno, 2020). To determine whether the selected inhibitors retained their activity in the aforementioned cell lines, we tested nitroxoline, compound **17**, compound **3**, and GCV-5 in Calu-3 cells and Vero E6 cells using the viral yield reduction assay. The results were compared with those obtained in Huh7-hACE2 cells (Table 2). Both CatB inhibitors, nitroxoline and compound **17**, showed a decrease of SARS-CoV-2 infection in Calu-3 and Vero E6 cells (Figure 2). Nitroxoline showed an EC_{50} value of 18.6 ± 10 μM for Vero E6 cells and an EC_{50} value of 23.3 ± 4.3 μM for Calu-3 cells, which was 10-fold higher than in Huh7-hACE2 (EC_{50} 1.9 ± 1.0 μM). Similarly, compound **17**, a more potent and selective inhibitor of CatB, showed very similar activity in Vero E6 and Calu-3 cells with EC_{50} values of 13.5 ± 0.6 μM and 14.4 ± 2.7 μM, respectively, however the activity was still lower compared to that of Huh7-hACE2 cells (EC_{50} 2.3 ± 0.4 μM) (Figure 2). Compound **3** inhibited SARS-CoV-2 infection in Vero E6 cells (Figure 3A) less effectively than in Calu-3 cells (Figure 3B), with EC_{50} values of 37.7 ± 10 μM and 12.4 ± 0.07, respectively (Table 2). Compound **3** is a less selective CatB inhibitor that targets other cathepsins including CatL and CatH, (our unpublished data) (Mirković et al., 2011; Mitrović et al., 2016). EC_{50} values for nitroxoline were comparable in Calu-3 and Vero E6 cells, although an order of magnitude higher than in Huh7-ACE2 cells. While for compound **3** EC_{50} values for Huh7-hACE2 and Calu-3 cells were at the same range and were higher for Vero E6 cells Table 2). Additionally, to evaluate the contribution of CatL in these cells, we used CatL inhibitor GCV-5. The results showed poor EC_{50} values for GCV-5. However, the compound still reduced by 100% the infection in Vero E6 cells and Calu-3 cells, whereas not even 50% reduction of the infection could be achieved in Huh7-hACE2 (Figure 2). Cell cytotoxicity was not detected at these concentrations (Figure S3). These data confirm that sensitivity to cathepsin inhibitors during SARS-CoV-2 infection depends on the cell type.

Nitroxoline, a drug with repurposing potential, was also tested in human primary cells derived from the upper or lower respiratory tract (Supplementary Figure S4). In both HNEpC and HPAEpC antiviral activity was observed in the low micromolar (EC_{50} ~5μM) with cytotoxicity at lower concentrations compared to cell lines (CC_{50} > 50 μM).

Table 2. Antiviral activity of cathepsin inhibitors at different cells lines

	Calu-3[a]			Huh7-hACE2			Vero E6		
	EC_{50}[b] **µM** (mean± SD[c])	EC_{90}[d] **µM** (mean± SD)	CC_{50}[e] **µM**	EC_{50} **µM** (mean± SD)	EC_{90} **µM** (mean± SD)	CC_{50} **µM**	EC_{50} **µM** (mean ± SD)	EC_{90} **µM** (mean± SD)	CC_{50} **µM**
Nitroxoline	23.3 ±4.3	n.a*	>100	1.9 ± 1.0	3.5 ± 0.4	>100	18.6 ± 10	52.4± 3.5	>100
Compound 17	14.4± 2.7	46.8 ± 4.4	>100	2.3 ± 0.4	4.0 ± 0.3	>100	13.5 ± 0.6	24.4± 0.0	>100
Compound 3	12.45 ± 0.07	18.8 ± 6.0	>100	10.7± 2.0	18.0 ± 7.5	>100	37.7 ±10	n.a*	>100
GCV-5	15.5 ± 13	50.0 ± 0.0	>100	n.a*	n.a*	>100	21.9± 2.2	27.1± 1.2	>100

*n.a : not assessable

[a] Cell type used to measure compound activity by the virus yield reduction assay

[b] Half maximal effective concentration obtained by the virus yield reduction assay

[c] Standard deviation

[d] Maximal effective concentration obtained by the virus yield reduction assay

[e] Half maximal cytotoxicity concentration obtained by the viability assay Alarmar Blue

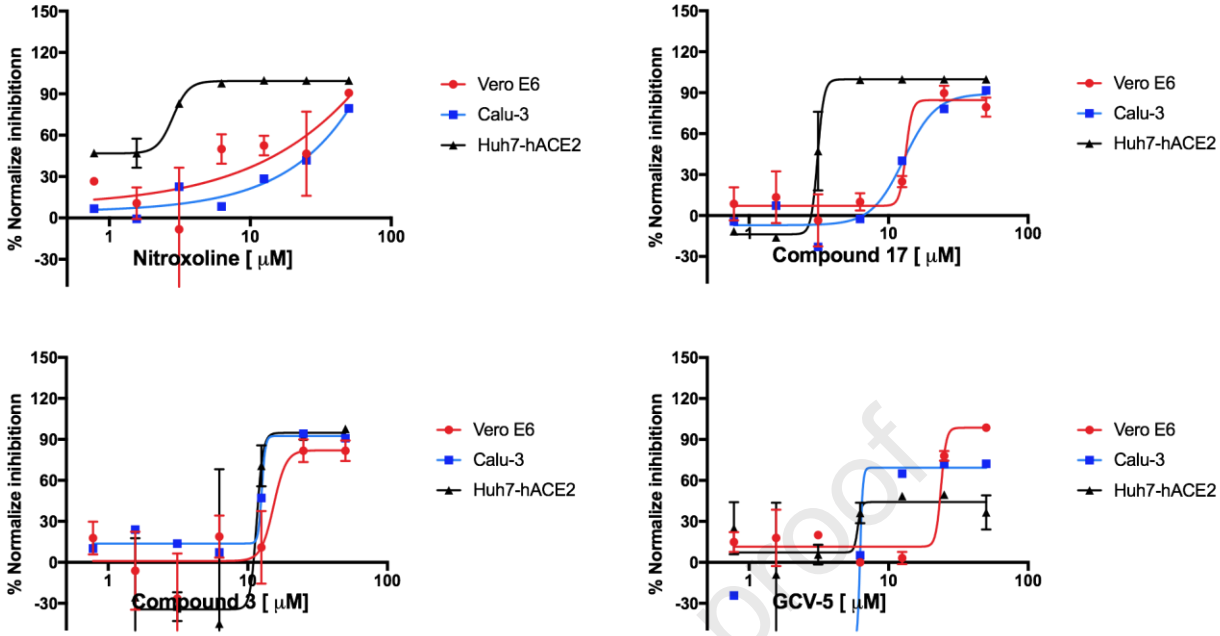

Figure 2. Activity of cathepsin inhibitors against SARS-CoV-2 D614G in different cells. Cells were treated with 2-fold dilutions of the inhibitors within a range of concentrations of 50 to 0.78 μM. The percentage of inhibition of virus yield was quantified by plaque assay. The black, blue, and red curves represent inhibition in Huh7-hACE2, Calu-3 and Vero E6 cells.

3.3 Expression and activity levels of CatB and CatL in different cells

To explain the antiviral effect of the inhibitors on selected cell lines, the protein levels and activity of CatB and CatL were determined in Vero E6, Huh7-hACE2, and Calu-3 cells. As shown by Western blot analysis (Figure 3A) and ELISA (Figure 3B), all cell lines contain CatB. Protein level of CatB was the highest in Calu-3 cells, followed by Huh7-hACE2 and Vero E6 cells. In all cell lines, CatB is present in all three forms: pro-CatB, active single-chain CatB and double-chain CatB. In line with this, the highest endo- and exopeptidase activity of CatB was observed in Calu-3 cells (Figure 3C). In Huh7-hACE2 cells, lower endo- and exopeptidase activity of CatB correlated with lower protein levels, whereas in Vero E6 cells, higher activity of CatB was observed than would have been expected from the protein levels (Figure 3C). The enzyme kinetics results show that CatB predominantly acts as endopeptidase in Vero E6 cells. The highest protein levels as well as the highest activity for CatL were observed in Vero E6 cells, compared to other two cell lines (Figure 3). The fluorogenic substrate Z-Phe-Arg-AMC was used to measure CatL activity. However, as this substrate is not specific for CatL but can also be degraded by CatB, the potent CatB-specific inhibitor CA-074 was added to the cell lysates in the assay to distinguish between substrate degradation due to CatL or due to CatB (Figure 3C). In Huh7-hACE2 and Calu-3 cells, in which higher protein levels and higher activity of CatB were detected, substrate degradation was almost completely abolished by the addition of CA-074, suggesting that Z-Phe-Arg-AMC substrate was degraded predominantly by CatB in these cells. In contrast, addition of CA-074 to Vero E6 cells' lysates did not reduce substrate degradation, indicating that CatL activity is responsible for substrate degradation. Considering the high levels of CatL protein and activity in Vero E6 cells compared to CatB, CatL might contribute in part to CatB substrate degradation. This could explain the apparent high activity of CatB observed in Vero E6 cells, which does not match protein concentration. These results are consistent with the antiviral effect of CatL inhibitors in Vero E6 cells, whereas their impact in other cell lines is weaker (Figure 2). These data suggest that SARS-CoV-2 may take advantage of different cathepsins for cell entry depending on their expression and activity.

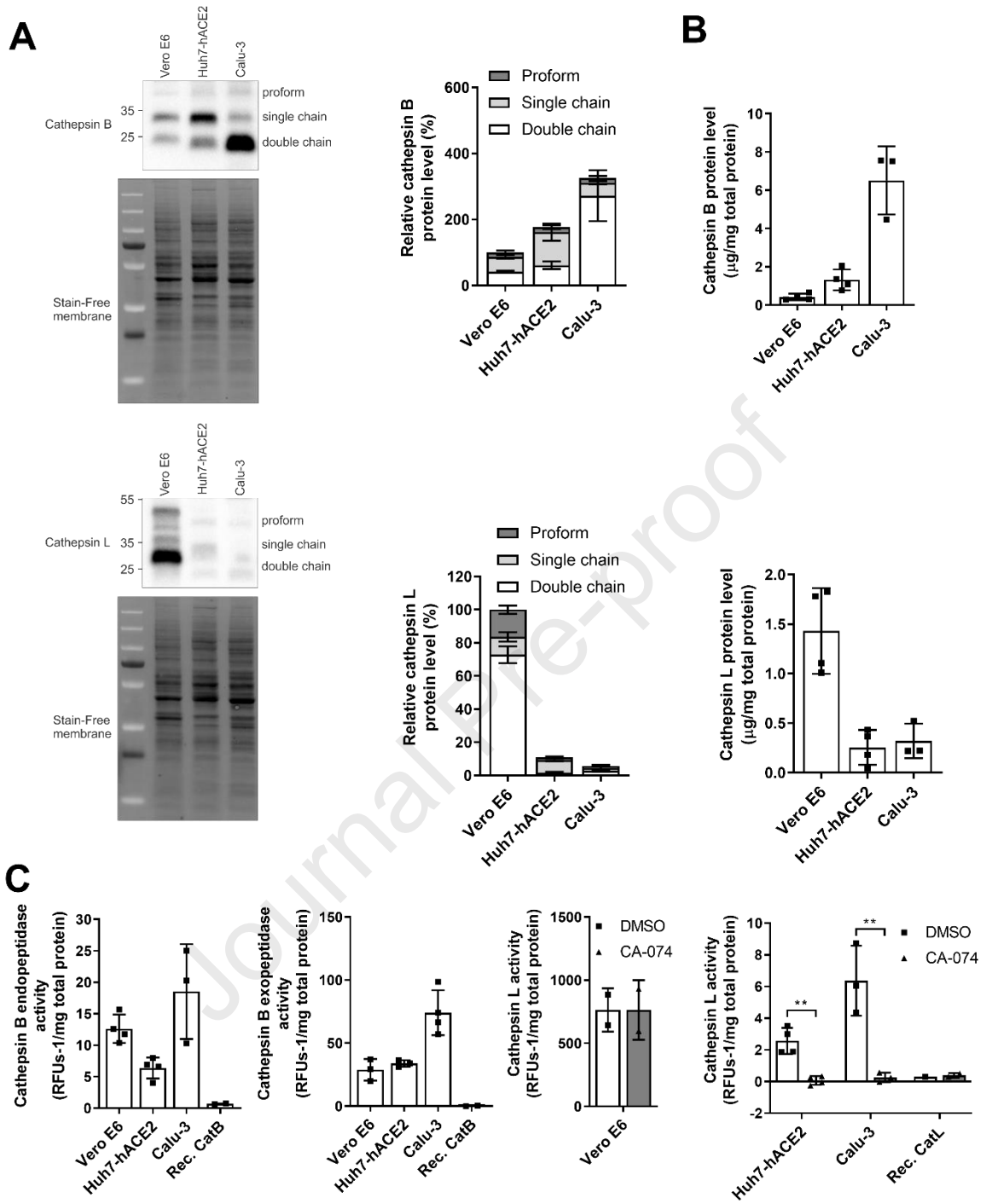

Figure 3. Expression and activity levels of CatB and CatL in different cell lines.

(**A**) CatB and CatL protein levels in whole-cell lysates of Vero E6, Huh7-hACE2, and Calu-3 cells as determined by Western blot analysis. Histograms show relative protein levels of CatB and CatL, with the contribution of each form indicated. Data are presented as mean ± SD.

(**B**) CatB and CatL protein levels in whole cell lysates as determined by ELISA. Data are given as mean ± SD.

(**C**) Activity of CatB and CatL in whole cell lysates assessed by enzyme kinetics using fluorogenic substrates. For specific assessment of CatL activity, CatB specific inhibitor CA-074 (10 μM) was added to exclude contribution of CatB to the degradation of the Z-Phe-Arg-AMC substrate. Data are presented as mean ± SD. $^{**}P < 0.01$.

3.4 The antiviral activity of cathepsin inhibitors is limited to early stages of viral infection.

Cathepsins are responsible for processing and cleavage of viral S protein in endosomes during entry, allowing the virus to release the nucleocapsid into the cytoplasm (Jackson et al., 2022; Padmanabhan et al., 2020; Pišlar et al., 2020; Schornberg et al., 2006). To assess the mode of action of cathepsin inhibitors, a time of addition experiment was performed. Huh7-hACE2 cells were treated at different times before or during infection (-3 h, 0 h, +1 h, +3 h, +5 h, and +18 h) (Figure 4A). The compounds that showed the highest antiviral activity in Huh7-hACE2 (Figure 1), such as nitroxoline, compound **17** and compound **3**, were selected to perform the time of addition studies and used at a final concentration of 10 μM.

All compounds significantly impaired viral infection when they were added shortly after infection (+1 h) and for up to 5 h after infection, consistent with cathepsins' activity in the early stages of infection (Figure 4B). Compound **3** showed the impact also when it was added before infection and at the time of infection. Furthermore, compound **17** impaired viral infection when it was added at the time of infection and also maintained antiviral activity at a later stage of infection as it significantly impaired viral infection also 18 h post-infection. The dosage regimen for nitroxoline treatment of urinal infections maintains active plasma concentrations of 10 μM (Mrhar et al., 1979; Naber et al., 2014; Wagenlehner et al., 2014; Wijma et al., 2018), which matches the EC_{90} values obtained thus ensuring the correct dosage also for the inhibition of SARS-CoV-2 infection.

A binding assay was performed to distinguish between virus adsorption and the later endocytosis and fusion steps. As shown in Figure 5A, virus absorption at 4 °C was not affected by the compounds (Figure 5A). Conversely, the entry assay showed that nitroxoline, compounds **3** and **17**, inhibited this step similarly to HCQ, a known inhibitor of virus endocytosis (Figure 5B). These data confirm the inhibitory effect of inhibitors during virus entry.

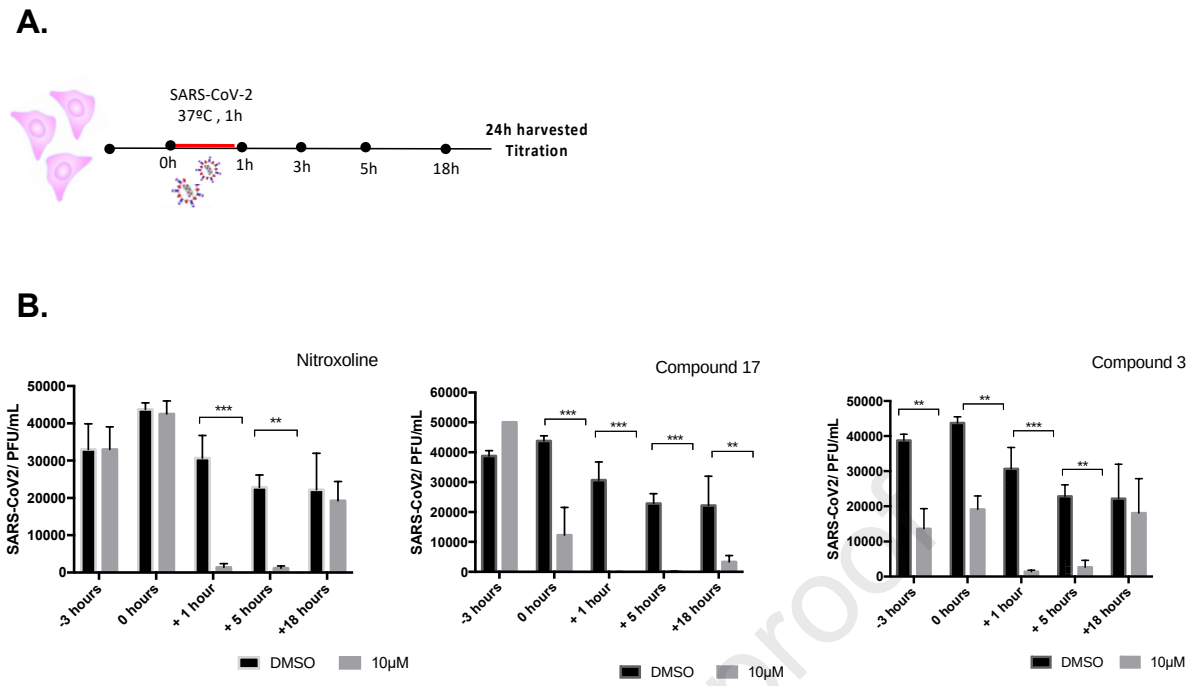

Figure 4. Evaluation of the effect of cathepsin inhibitors at different stages of SARS-CoV2 D614G infection in Huh7-hACE2 cells.

(**A**) Diagram of the experimental setup showing the time points when the compounds were added at a concentration of 10 µM, SARS-CoV-2 was inoculated at time 0 for 1 hour at MOI 0.1.

(**B**) Viral yields for nitroxoline, compound **17** and compound **3**. DMSO-treated samples were used as control. Bars represent mean ± SD of two replicates. **P* ≤ 0.05, ***P* ≤ 0.01, ****P* ≤ 0.001, *****P* ≤ 0.0001 (two-way ANOVA, followed by Sidak's test).

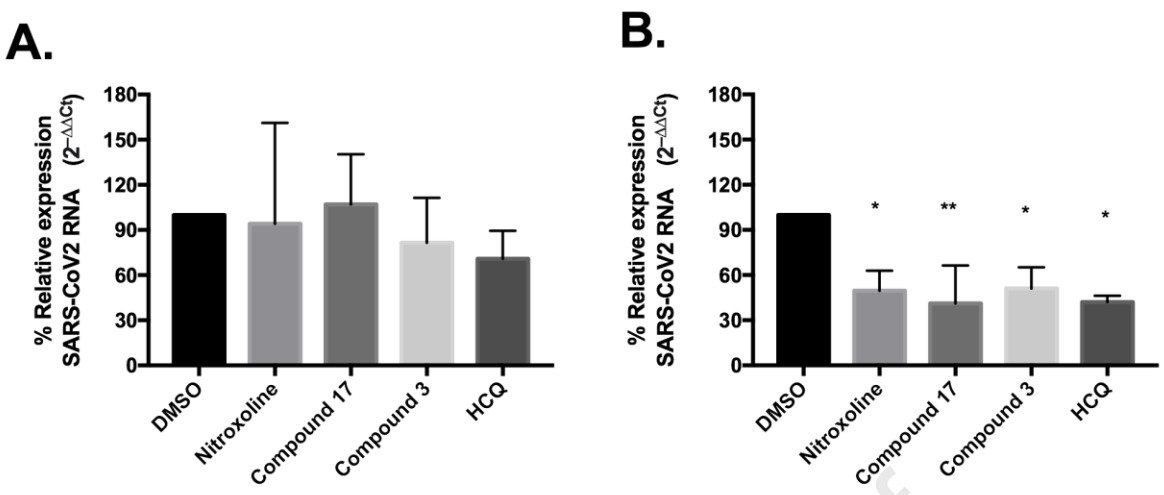

Figure 5. Effect of nitroxoline, compound 17, and compound 3 on the binding or endocytosis/fusion of SARS-CoV-2.

(A) Binding assay monitored on Huh7-hACE2 treated with the viral inoculum (SARS-CoV-2 at MOI 2) and 20 μM cathepsin inhibitors, 20 μM HCQ (positive control) or 1% DMSO as a negative control for 2 h at 4 °C. Cells were then washed with ice-cold PBS and extracted to determine viral RNA by real time (RT)qPCR. The housekeeping gene GAPDH was used as a reference. Viral genomes are expressed as percentage of relative expression (double-delta Ct method) compared with the negative control (DMSO without transduction). Bars represent mean ± SD from two replicates of independent experiment. $*P \leq 0.033$, $**P \leq 0.002$, $***P \leq 0.001$ (one-way ANOVA followed by Dunnett's test).

(B) Entry assay monitored on Huh7-hACE2 treated with the viral inoculum (SARS-CoV-2 at MOI 2) at 4 °C for 2 h. After 2 h, cells were washed with PBS and supplemented with fresh medium containing 2% FBS and 20 μM cathepsin inhibitors, 20 μM HQC or 1% DMSO. Cells were maintained at 37 °C for 3 h. Cells were then processed as described above (Figure 5A).

3.5 Activity of CatB and CatL inhibitors against the SARS-CoV2 Omicron variant

Since the end of 2021, the SARS-CoV-2 Omicron variant B.1 and its sub-lineages are prevalent worldwide (2022; WHO, 2021). Previous work has shown that the SARS-CoV-2 B.1 variant enters cells via the endocytosis pathway, independent of the TMPRRS2 protease. In this context, cathepsins play an important role in SARS-CoV-2 infection (Meng et al., 2022; Willett et al., 2022; Zhao et al., 2022). Therefore, we evaluated the inhibitory effect of cathepsin inhibitors against SARS-CoV-2 Omicron variant B.1. Effect of nitroxoline, compound **17**, compound **3**, GCV-5, E-64 and its cell permeable derivative E-64d was evaluated using HCA on Huh7-hACE2. After 72 h, infection was measured by assessing nucleocapsid structural protein (N) expression (Figure 6A). Nitroxoline, compound **17**, and compound **3** showed an EC_{50} values 4.1 ± 0.7 μM, 6.6 ± 0.4 μM and 5.4 ± 0.8 μM, respectively (Table 3). Interestingly general cathepsin inhibitors, such as E-64 and E-64d also demonstrated a dose-response antiviral activity against this viral variant with EC_{50} values 4.3 ± 1.2 μM and 1.1 ± 0,44 μM, respectively. However, the specific CatL inhibitor, GCV-5, was confirmed cytotoxic in these cells. These data indicate that the cathepsin inhibitors are also effective against the Omicron variant and suggest that the virus evolved to modify the use of cathepsins to promote cell entry.

Table 3. Dose-response results from cathepsin inhibitors in Huh7-hACE2 infected with SARS-CoV-2 Omicron

	EC_{50} [a] **µM (mean± SD [b])**	EC_{90} [c] **µM (mean± SD)**	CC_{50} [d] **µM**	**Highest % of Virus Inhibition**
Nitroxoline	4.1±0.7	6.4±0.6	>100	100
Compound 17	6.6±0.4	14.7± 9.8	>100	98
Compound 03	5.4± 0.8	6.8 ±0.4	>100	100
E64	4.3 ±1.16	14.9 ±0.0	> 100	91
E64-d	1.1 ± 0.44	n.a*	> 100	83
GVC-5	n.a*	n.a*	n.a*	n.a*
Hidroxychloroquine[e]	2.6± 0.36	7.7 ± 1.2	>100	99

*n.a not assessable

[a]Half maximal effective concentration from values obtained in HCA

[b] Standard deviation

[c] Maximal effective concentration from values obtained in HCA

[d] Half maximal cytotoxic concentration from values obtained in HCA

[e] Reference compound, positive control

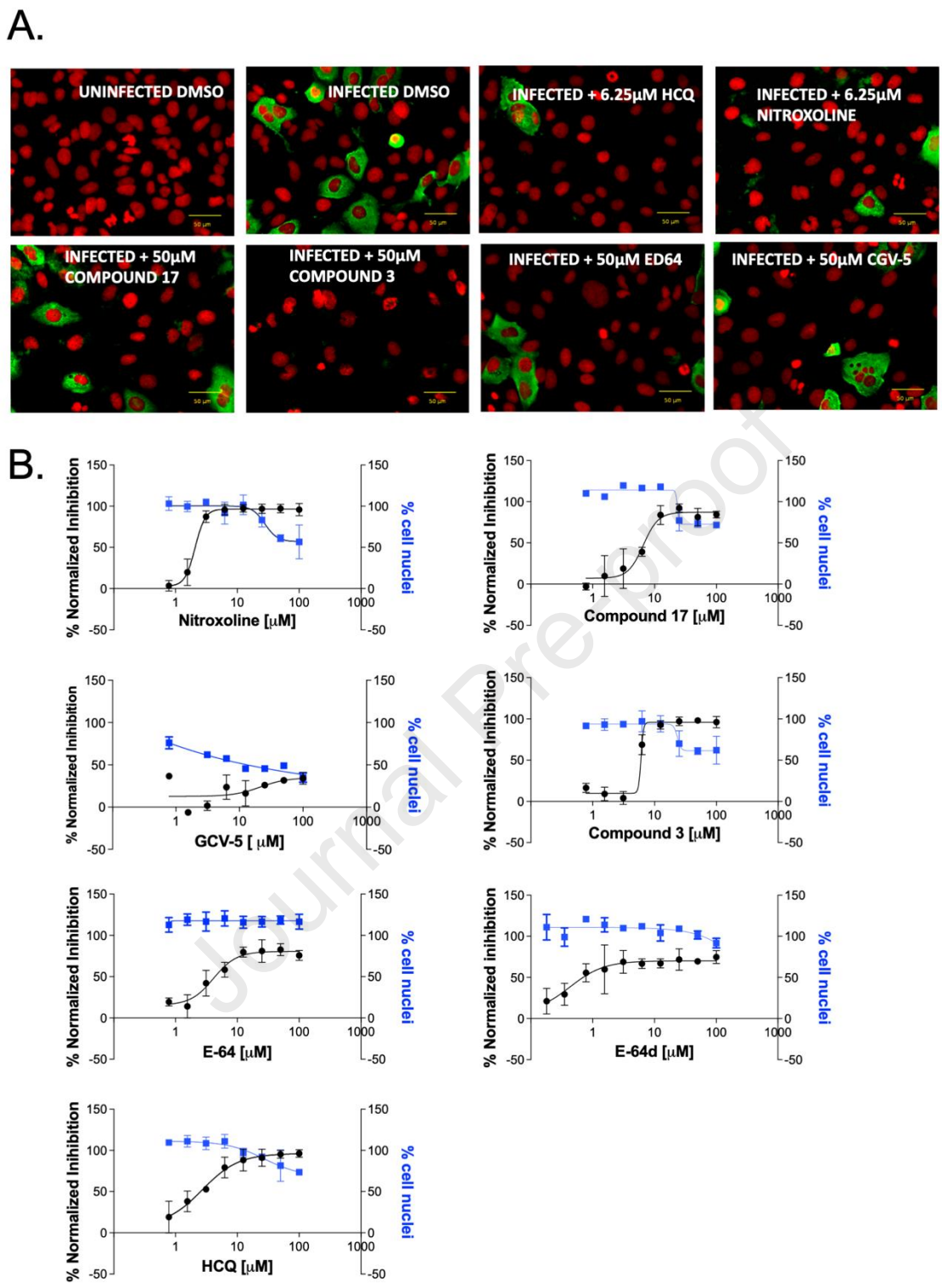

Figure 6. Cathepsin inhibitors are effective against the SARS-CoV-2 Omicron variant. (**A**) Representative images from High Content assay (HCA) showing infection of SARS-CoV-2 Omicron in Huh7-hACE2 at 24 h. Cells were infected and treated with the inhibitors simultaneously for 24 h. Then cells were fixed and processed for immunofluorescence with the anti-nucleocapsid antibody (green fluorescence). Nuclei were stained with DAPI (red

fluorescence). Plates from HCA were imaged, and image analysis was performed using the High Content System microscope.

(**B**) Dose-response of cathepsin inhibitors against SARS-CoV-2 Omicron in Huh7-hACE2. Hydroxychloroquine (HQC) was used as a reference compound. Plates from HCA were acquired, and image analysis was performed using the High Content System microscope. The percentage of inhibition (black dots) was calculated from image analysis after normalization with the average infection ratio of cells treated with 1% DMSO. The percentage of nuclei (blue triangles) was normalized by the total number of cells.

3. Discussion

Drugs that target viral and host factors essential for virus entry, replication, and spread are in need to overcome new pandemic threats (Chitsike and Duerksen-Hughes, 2021; Fang, 2022). Cathepsins, have been identified as important host factors involved in the endosome-dependent entry pathway of viruses, including SARS-CoV-2 (Evans and Liu, 2021; Hoffmann et al., 2020; Pišlar et al., 2020; Shang et al., 2020). Cathepsins are druggable enzymes and we identified the antibiotic nitroxoline as a potent, selective and reversible inhibitor of CatB (Kos et al., 2014). Pharmacokinetic and toxicity data are available for nitroxoline (Mrhar et al., 1979; Naber et al., 2014; Wagenlehner et al., 2014; Wijma et al., 2018), which is administered orally for the treatment of urinary infection. Nitroxoline and its derivative compound **17**, with improved potency and selectivity for CatB (Mitrović et al., 2017; Sosič et al., 2013), reduced SARS-CoV-2 D614G infection by more than 90% in Huh7-hACE2 (Table I, Figure 1). Another nitroxoline derivative, compound **3**, which has a larger structural element that decreases its selectivity and potency for inhibiting CatB activity and increases inhibitory activity against CatL (Mirković et al., 2011; Mitrović et al., 2016), also showed high antiviral activity with EC_{50} values of less than 10 μM (Table I, Figure 1). In contrast, treatment with inhibitors selective for CatL, compounds CLIK-148 (Katunuma et al., 1999) and GCV-5 (Mitrović et al., 2022), had weaker antiviral activity (CLIK-148) or failed (GCV-5) to reduce SARS-CoV-2 infection (Table I). These results highlight the role of CatB in the endosomal-dependent pathway of SARS-CoV-2 infection in Huh7-hACE2 cells.

Targeted cathepsins are mainly involved in endosomal-dependent cell entry and less in further steps of viral replication and propagation (Figure 4) (Jackson et al., 2022; Padmanabhan et al., 2020; Pišlar et al., 2020; Schornberg et al., 2006). This was also confirmed by the binding assay, where none of the inhibitors affected viral adsorption, while all of them significantly inhibited endocytosis step during viral entry (Figure 5). Only compound **17** retained some antiviral activity also at later stages of infection indicating that other functions cannot be completely excluded (Figure 4).

The role of either CatB or CatL in S protein processing during SARS-CoV-2 entry is being actively investigated. Studies consistent with our findings confirmed the importance of CatB during SARS-CoV-2 infection. The work of Hashimoto suggests that CatB plays an important role in endocytosis-dependent infection reinforced by the antiviral activity of CatB inhibitor CA-074Me (Hashimoto et al. 2021). Another study performed on lung tissue from cancer patients infected with SARS-CoV-2 showed that CatB expression increased after virus infection and is associated with a hyperinflammatory response and poor prognosis (Ding et al., 2022).Cat

B inhibitors could therefore have a dual effect, impairing viral uptake and excessive inflammation, as suggested for Cat L inhibitors (Mellott et al., 2021; Wu et al., 2020; Zhao et al., 2021). In contrast, other studies show that CatL plays an essential role in SARS-CoV-2 endosome-dependent entry into Hek293T-hACE2 cells (Ou et al., 2020; Zhou et al., 2016; Zhou et al., 2015). For example, treatment with a CatL inhibitor reduced entry of SARS-CoV-2 by more than 76%, in these cells, while no effect on virus entry was observed after treatment with a CatB inhibitor (Ou et al., 2020). CatL, rather than CatB, was reported to cleave SARS-CoV-2 Spike, at pH 5.5 (Mellott et al., 2021). However, at this low pH the endopeptidase activity of CatB is sub-optimal and CatB-mediated Spike cleavage has been previously reported (Bollavaram et al., 2021; Jaimes et al., 2020). In addition, most of the reports showing little effect for CatB were performed in HEK-293-hACE2 or Vero E6 cell lines (Ashhurst et al., 2022; Mediouni et al., 2022; Ou et al., 2021; Ou et al., 2020). We therefore compared the different cell models showing that the antiviral activity of the cathepsin inhibitors correlated with the protein levels and activity of both cathepsins in each cell line used in the assay (Figure 3). For nitroxoline and its two derivatives, compound **17** and compound **3**, the strongest antiviral effect was observed in the Huh7-hACE2 cell line containing a high content of active CatB (Figure 3). Addition of a potent irreversible CatB specific inhibitor CA-074 to discriminate between CatB and CatL activity showed that CatB dominated over CatL in this cell line (Figure 3). In the other two cell lines used, Calu-3 and Vero E6, nitroxoline and compound **17** were found to be approximately 10-fold and 5-fold less potent, respectively, compared with Huh7-hACE2 cells (Figure 2). The differences in inhibitor antiviral efficacy could be explained by the differences in protein levels and activity of CatB and CatL. In Calu-3 cells, protein levels and activity of CatB were higher than in Huh7-hACE2 cells. Because EC_{50} values are kinetic parameters, dependent on the experimental settings, including the concentration of enzyme and substrate in the assay (Copeland, 2005), a higher concentration of CatB inhibitor is required in Calu-3 to achieve the same inhibitory effect as in Huh7-hACE2 cells. Moreover, Calu-3 cells predominantly support the membrane fusion entry pathway due to their high endogenous expression of TMPRSS2 (Hoffmann et al., 2020; Ou et al., 2021; Saccon et al., 2021), which can additionally reduce the overall effect of CatB inhibitors. In contrast, in Vero E6 cells, the protein and activity levels of CatL are much higher than CatB indicating that CatL plays the major role during SARS-CoV-2 Spike cleavage and consequently cell entry and this could be a reason for the lower effect of CatB inhibitors in this host cell type compared to others. Moreover, the addition of the CatB specific inhibitor CA-074 in this cell line had no additional effect on CatL substrate degradation. Together, these data explain the

lower effect of the CatB inhibitors nitroxoline and compound **17** on inhibition of SARS-CoV-2 infection in Vero E6 cells. These results may also explain the lack of effect of CatB inhibitors reported in some other studies that used this cell model (Ashhurst et al., 2022; Mediouni et al., 2022; Ou et al., 2021). The inhibition of SARS-CoV-2 infection by compound **3** did not correlate so well with the protein levels and activity of both CatB and CatL compared to nitroxoline and compound **17**. In this regard it should be noted that compound **3** is an equal inhibitor of both, CatB and CatL, but less potent compared to nitroxoline and compound **17**. To confirm our hypothesis about the correlation of cathepsin expression and compound efficacy in inhibiting SARS-CoV-2 infection, we next tested the effect of the specific CatL inhibitor GCV-5. In line with other studies, this compound is active in Vero E6 cells infected with SARS-CoV-2 (Ashhurst et al., 2022; Mellott et al., 2021).

The Omicron variant of SARS-CoV-2 was sensitive to CatB inhibitors (Figure 6). Omicron enters the cells mainly via the endosomal pathway, and is more sensitive to host cathepsins compared to previous variants (Benlarbi et al., 2022; Du et al., 2022; Hu et al., 2022; Hui et al., 2022; Meng et al., 2022; Willett et al., 2022). Indeed, E-64d was more effective also in our case (Table 3). Mutations within the Omicron S protein that alter conformation and interactions with the receptor, could affect utilization of different cathepsins for its entry thus modifying sensitivity to cathepsin inhibitors (Du et al., 2022; Hu et al., 2022; Hui et al., 2022; Imai et al., 2023; Willett et al., 2022). Selection of the proteolytic profile needed for virus entry into host cells is another level of adaptation of SARS-CoV-2 virus to its frequent genetic changes. Furthermore, differential cathepsin expression in tissues may dictate viral tropism and pathological consequences, as well as opportunities for specific inhibitors to impact on the consequences of infection on other tissues. For example, expression analysis shows that nasal epithelial cells are enriched for ACE2 not matched by TMPRSS2 levels, which seem to be compensated by CatL/CatB (Sungnak et al., 2020). In the human vasculature the expression pattern of CatB/CatL varies with CatB being mainly expressed in the brain vasculature and CatL predominantly in the peripheral vasculature, notably in the absence of TMPRSS2 expression in both cases (Ghobrial et al. BiorXiv doi.org/10.1101/2020.10.10.334664). Intriguingly, CatB is also expressed in microglia thus providing an interesting CatB-dependent pathway of entry that could account for long-term neuropathological consequences of COVID-19.

4. Conclusion

The results presented here highlight the important role of host cysteine CatB in SARS-CoV-2 virus entry and demonstrate that, in addition to CatL inhibitors, specific CatB inhibitors, such as nitroxoline and its derivatives, significantly impair SARS-CoV-2 infection. As they solely inhibit CatB endopeptidase activity, involved in virus entry and inflammation, they would less likely affect physiological function of CatB based on exopeptidase activity. Furthermore, our data suggest that the antiviral activity of the inhibitors correlates with the amount of targeted cathepsin in host cells and depends on cell type and viral adaptions. Overall, the use of cathepsin-specific inhibitors could serve as a reliable therapeutic strategy against SARS-CoV-2 infection. Other polypharmacological effects of Cat inhibitors on SARS-CoV-2 induced inflammation could be additional advantages of the approach that deserve to be explored in more detail. To note, nitroxoline would act as repurposed drug in this context being clinically used as an antibiotic. Further studies would be required to explore the clinical use of nitroxoline in the context of SARS-CoV-2 infection, including dosage *in vivo*, route of administration and side effects.

5. Declaration of competing interest

The authors declare the international application number PCT/EP2021/083960 "8-hydroxyquinoline cysteine protease inhibitors for use in the prevention and/or treatment of a corona virus disease". The authors declare that they have no known competing financial interests or personal relationships that could have appeared to influence the work reported in this paper.

6. Funding

This work was supported by the Slovenian Research Agency, grant numbers P4-0127 to J.K., J3-3071 to AnM, and P1-0208 to SG. Work in AM laboratory related to SARS-CoV-2 is supported by grants from SNAM Foundation, Generali SpA, Beneficentia Stiftung, CARIPLO (INNATE-CoV) and the #FarmaCovid crowdfunding initiative. The funders had no role in the study design, data collection and analysis, or preparation of the manuscript.

7. References

Ashhurst, A.S., Tang, A.H., Fajtová, P., Yoon, M.C., Aggarwal, A., Bedding, M.J., Stoye, A., Beretta, L., Pwee, D., Drelich, A., Skinner, D., Li, L., Meek, T.D., McKerrow, J.H., Hook, V., Tseng, C.-T., Larance, M., Turville, S., Gerwick, W.H., O'Donoghue, A.J., Payne, R.J., 2022. Potent Anti-SARS-CoV-2 Activity by the Natural Product Gallinamide A and Analogues via Inhibition of Cathepsin L. Journal of Medicinal Chemistry 65, 2956-2970.

Benlarbi, M., Laroche, G., Fink, C., Fu, K., Mulloy, R.P., Phan, A., Ariana, A., Stewart, C.M., Prevost, J., Beaudoin-Bussieres, G., Daniel, R., Bo, Y., El Ferri, O., Yockell-Lelievre, J., Stanford, W.L., Giguere, P.M., Mubareka, S., Finzi, A., Dekaban, G.A., Dikeakos, J.D., Cote, M., 2022. Identification and differential usage of a host metalloproteinase entry pathway by SARS-CoV-2 Delta and Omicron. iScience 25, 105316.

Bollavaram, K., Leeman, T.H., Lee, M.W., Kulkarni, A., Upshaw, S.G., Yang, J., Song, H., Platt, M.O., 2021. Multiple sites on SARS-CoV-2 spike protein are susceptible to proteolysis by cathepsins B, K, L, S, and V. Protein Sci 30, 1131-1143.

Cagno, V., 2020. SARS-CoV-2 cellular tropism. The Lancet Microbe 1, e2-e3.

Chandran, K., Sullivan, N.J., Felbor, U., Whelan, S.P., Cunningham, J.M., 2005. Endosomal proteolysis of the Ebola virus glycoprotein is necessary for infection. Science (New York, N.Y.) 308, 1643-1645.

Chitsike, L., Duerksen-Hughes, P., 2021. Keep out! SARS-CoV-2 entry inhibitors: their role and utility as COVID-19 therapeutics. Virology Journal 18, 154-154.

Copeland, R.A., 2005. Evaluation of enzyme inhibitors in drug discovery: a guide for medicinal chemists and pharmacologists. Wiley-Interscience, New York.

CoVariants, 2022. https://covariants.org (accessed December 2022).

Dana, D., Pathak, S.K., 2020. A review of small molecule inhibitors and functional probes of human cathepsin L.

Diederich, S., Thiel, L., Maisner, A., 2008. Role of endocytosis and cathepsin-mediated activation in Nipah virus entry. Virology 375, 391-400.

Ding, X., Ye, N., Qiu, M., Guo, H., Li, J., Zhou, X., Yang, M., Xi, J., Liang, Y., Gong, Y., Li, J., 2022. Cathepsin B is a potential therapeutic target for coronavirus disease 2019 patients with lung adenocarcinoma. Chemico-Biological Interactions 353, 109796-109796.

Dolgin, E., 2021. The race for antiviral drugs to beat COVID — and the next pandemic. Nature 592, 340-343.

Du, X., Tang, H., Gao, L., Wu, Z., Meng, F., Yan, R., Qiao, S., An, J., Wang, C., Qin, F.X.-F., 2022. Omicron adopts a different strategy from Delta and other variants to adapt to host. Signal Transduction and Targeted Therapy 7, 45-45.

Evans, J.P., Liu, S.-L., 2021. Role of host factors in SARS-CoV-2 entry. Journal of Biological Chemistry 297, 100847-100847.

Fang, F.F., 2022. As the virus evolves, so too must we: a drug developer's perspective. Virology Journal 19, 159-159.

Gomes, C.P., Fernandes, D.E., Casimiro, F., da Mata, G.F., Passos, M.T., Varela, P., Mastroianni-Kirsztajn, G., Pesquero, J.B., 2020. Cathepsin L in COVID-19: From Pharmacological Evidences to Genetics. Frontiers in Cellular and Infection Microbiology 10.

Gottlieb, R.L., Vaca, C.E., Paredes, R., Mera, J., Webb, B.J., Perez, G., Oguchi, G., Ryan, P., Nielsen, B.U., Brown, M., Hidalgo, A., Sachdeva, Y., Mittal, S., Osiyemi, O., Skarbinski, J., Juneja, K., Hyland, R.H., Osinusi, A., Chen, S., Camus, G., Abdelghany, M., Davies, S., Behenna-Renton, N., Duff, F., Marty, F.M., Katz, M.J., Ginde, A.A., Brown, S.M., Schiffer, J.T., Hill, J.A., 2022. Early Remdesivir to Prevent Progression to Severe Covid-19 in Outpatients. New England Journal of Medicine 386, 305-315.

Hoffmann, M., Kleine-Weber, H., Schroeder, S., Krüger, N., Herrler, T., Erichsen, S., Schiergens, T.S., Herrler, G., Wu, N.-H.H., Nitsche, A., Müller, M.A., Drosten, C., Pöhlmann, S., 2020. SARS-CoV-2 Cell Entry Depends on ACE2 and TMPRSS2 and Is Blocked by a Clinically Proven Protease Inhibitor. Cell 181, 271-280.e278.
Hu, B., Chan, J.F.-W., Liu, H., Liu, Y., Chai, Y., Shi, J., Shuai, H., Hou, Y., Huang, X., Yuen, T.T.-T., Yoon, C., Zhu, T., Zhang, J., Li, W., Zhang, A.J., Zhou, J., Yuan, S., Zhang, B.-Z., Yuen, K.-Y., Chu, H., 2022. Spike mutations contributing to the altered entry preference of SARS-CoV-2 omicron BA.1 and BA.2. Emerging Microbes & Infections 11, 2275-2287.
Hui, K.P.Y., Ho, J.C.W., Cheung, M.-c., Ng, K.-c., Ching, R.H.H., Lai, K.-l., Kam, T.T., Gu, H., Sit, K.-Y., Hsin, M.K.Y., Au, T.W.K., Poon, L.L.M., Peiris, M., Nicholls, J.M., Chan, M.C.W., 2022. SARS-CoV-2 Omicron variant replication in human bronchus and lung ex vivo. Nature 603, 715-720.
Imai, M., Ito, M., Kiso, M., Yamayoshi, S., Uraki, R., Fukushi, S., Watanabe, S., Suzuki, T., Maeda, K., Sakai-Tagawa, Y., Iwatsuki-Horimoto, K., Halfmann, P.J., Kawaoka, Y., 2023. Efficacy of Antiviral Agents against Omicron Subvariants BQ.1.1 and XBB. New England Journal of Medicine 388, 89-91.
Jackson, C.B., Farzan, M., Chen, B., Choe, H., 2022. Mechanisms of SARS-CoV-2 entry into cells. Nature Reviews Molecular Cell Biology 23, 3-20.
Jaimes, J.A., Millet, J.K., Whittaker, G.R., 2020. Proteolytic Cleavage of the SARS-CoV-2 Spike Protein and the Role of the Novel S1/S2 Site. iScience 23, 101212.
Jayk Bernal, A., Gomes da Silva, M.M., Musungaie, D.B., Kovalchuk, E., Gonzalez, A., Delos Reyes, V., Martín-Quirós, A., Caraco, Y., Williams-Diaz, A., Brown, M.L., Du, J., Pedley, A., Assaid, C., Strizki, J., Grobler, J.A., Shamsuddin, H.H., Tipping, R., Wan, H., Paschke, A., Butterton, J.R., Johnson, M.G., De Anda, C., 2022. Molnupiravir for Oral Treatment of Covid-19 in Nonhospitalized Patients. New England Journal of Medicine 386, 509-520.
Katunuma, N., Murata, E., Kakegawa, H., Matsui, A., Tsuzuki, H., Tsuge, H., Turk, D., Turk, V., Fukushima, M., Tada, Y., Asao, T., 1999. Structure based development of novel specific inhibitors for cathepsin L and cathepsin S in vitro and in vivo. FEBS Letters 458, 6-10.
Kawase, M., Shirato, K., Matsuyama, S., Taguchi, F., 2009. Protease-Mediated Entry via the Endosome of Human Coronavirus 229E. Journal of Virology 83, 712-721.
Kokic, G., Hillen, H.S., Tegunov, D., Dienemann, C., Seitz, F., Schmitzova, J., Farnung, L., Siewert, A., Höbartner, C., Cramer, P., 2021. Mechanism of SARS-CoV-2 polymerase stalling by remdesivir. Nature Communications 12, 279-279.
Kos, J., Mitrović, A., Mirković, B., 2014. The current stage of cathepsin B inhibitors as potential anticancer agents. Future medicinal chemistry 6, 1355-1371.
Kos, J., Sekirnik, A., Premzl, A., Bergant, V.Z., Langerholc, T., Turk, B., Werle, B., Golouh, R., Repnik, U., Jeras, M., Turk, V., 2005. Carboxypeptidases cathepsins X and B display distinct protein profile in human cells and tissues. Experimental Cell Research 306, 103-113.
Licastro, D., Rajasekharan, S., Dal Monego, S., Segat, L., D'Agaro, P., Marcello, A., 2020. Isolation and Full-Length Genome Characterization of SARS-CoV-2 from COVID-19 Cases in Northern Italy. J Virol 94.
Liu, T., Luo, S., Libby, P., Shi, G.-P., 2020. Cathepsin L-selective inhibitors: A potentially promising treatment for COVID-19 patients. Pharmacology & Therapeutics 213, 107587-107587.
Marzi, M., Vakil, M.K., Bahmanyar, M., Zarenezhad, E., 2022. Paxlovid: Mechanism of Action, Synthesis, and In Silico Study. BioMed Research International 2022, 1-16.
Mediouni, S., Mou, H., Otsuka, Y., Jablonski, J.A., Adcock, R.S., Batra, L., Chung, D.-H., Rood, C., de Vera, I.M.S., Rahaim Jr, R., Ullah, S., Yu, X., Getmanenko, Y.A., Kennedy, N.M., Wang, C., Nguyen, T.-T., Hull, M., Chen, E., Bannister, T.D., Baillargeon, P.,

Scampavia, L., Farzan, M., Valente, S.T., Spicer, T.P., 2022. Identification of potent small molecule inhibitors of SARS-CoV-2 entry. SLAS Discovery 27, 8-19.
Mellott, D.M., Tseng, C.T., Drelich, A., Fajtova, P., Chenna, B.C., Kostomiris, D.H., Hsu, J., Zhu, J., Taylor, Z.W., Kocurek, K.I., Tat, V., Katzfuss, A., Li, L., Giardini, M.A., Skinner, D., Hirata, K., Yoon, M.C., Beck, S., Carlin, A.F., Clark, A.E., Beretta, L., Maneval, D., Hook, V., Frueh, F., Hurst, B.L., Wang, H., Raushel, F.M., O'Donoghue, A.J., de Siqueira-Neto, J.L., Meek, T.D., McKerrow, J.H., 2021. A Clinical-Stage Cysteine Protease Inhibitor blocks SARS-CoV-2 Infection of Human and Monkey Cells. ACS Chem Biol 16, 642-650.
Meng, B., Abdullahi, A., Ferreira, I.A.T.M., Goonawardane, N., Saito, A., Kimura, I., Yamasoba, D., Gerber, P.P., Fatihi, S., Rathore, S., Zepeda, S.K., Papa, G., Kemp, S.A., Ikeda, T., Toyoda, M., Tan, T.S., Kuramochi, J., Mitsunaga, S., Ueno, T., Shirakawa, K., Takaori-Kondo, A., Brevini, T., Mallery, D.L., Charles, O.J., Baker, S., Dougan, G., Hess, C., Kingston, N., Lehner, P.J., Lyons, P.A., Matheson, N.J., Ouwehand, W.H., Saunders, C., Summers, C., Thaventhiran, J.E.D., Toshner, M., Weekes, M.P., Maxwell, P., Shaw, A., Bucke, A., Calder, J., Canna, L., Domingo, J., Elmer, A., Fuller, S., Harris, J., Hewitt, S., Kennet, J., Jose, S., Kourampa, J., Meadows, A., O'Brien, C., Price, J., Publico, C., Rastall, R., Ribeiro, C., Rowlands, J., Ruffolo, V., Tordesillas, H., Bullman, B., Dunmore, B.J., Gräf, S., Hodgson, J., Huang, C., Hunter, K., Jones, E., Legchenko, E., Matara, C., Martin, J., Mescia, F., O'Donnell, C., Pointon, L., Shih, J., Sutcliffe, R., Tilly, T., Treacy, C., Tong, Z., Wood, J., Wylot, M., Betancourt, A., Bower, G., Cossetti, C., De Sa, A., Epping, M., Fawke, S., Gleadall, N., Grenfell, R., Hinch, A., Jackson, S., Jarvis, I., Krishna, B., Nice, F., Omarjee, O., Perera, M., Potts, M., Richoz, N., Romashova, V., Stefanucci, L., Strezlecki, M., Turner, L., De Bie, E.M.D.D., Bunclark, K., Josipovic, M., Mackay, M., Butcher, H., Caputo, D., Chandler, M., Chinnery, P., Clapham-Riley, D., Dewhurst, E., Fernandez, C., Furlong, A., Graves, B., Gray, J., Hein, S., Ivers, T., Le Gresley, E., Linger, R., Kasanicki, M., King, R., Kingston, N., Meloy, S., Moulton, A., Muldoon, F., Ovington, N., Papadia, S., Penkett, C.J., Phelan, I., Ranganath, V., Paraschiv, R., Sage, A., Sambrook, J., Scholtes, I., Schon, K., Stark, H., Stirrups, K.E., Townsend, P., Walker, N., Webster, J., Butlertanaka, E.P., Tanaka, Y.L., Ito, J., Uriu, K., Kosugi, Y., Suganami, M., Oide, A., Yokoyama, M., Chiba, M., Motozono, C., Nasser, H., Shimizu, R., Kitazato, K., Hasebe, H., Irie, T., Nakagawa, S., Wu, J., Takahashi, M., Fukuhara, T., Shimizu, K., Tsushima, K., Kubo, H., Kazuma, Y., Nomura, R., Horisawa, Y., Nagata, K., Kawai, Y., Yanagida, Y., Tashiro, Y., Tokunaga, K., Ozono, S., Kawabata, R., Morizako, N., Sadamasu, K., Asakura, H., Nagashima, M., Yoshimura, K., Cárdenas, P., Muñoz, E., Barragan, V., Márquez, S., Prado-Vivar, B., Becerra-Wong, M., Caravajal, M., Trueba, G., Rojas-Silva, P., Grunauer, M., Gutierrez, B., Guadalupe, J.J., Fernández-Cadena, J.C., Andrade-Molina, D., Baldeon, M., Pinos, A., Bowen, J.E., Joshi, A., Walls, A.C., Jackson, L., Martin, D., Smith, K.G.C., Bradley, J., Briggs, J.A.G., Choi, J., Madissoon, E., Meyer, K.B., Mlcochova, P., Ceron-Gutierrez, L., Doffinger, R., Teichmann, S.A., Fisher, A.J., Pizzuto, M.S., de Marco, A., Corti, D., Hosmillo, M., Lee, J.H., James, L.C., Thukral, L., Veesler, D., Sigal, A., Sampaziotis, F., Goodfellow, I.G., Matheson, N.J., Sato, K., Gupta, R.K., 2022. Altered TMPRSS2 usage by SARS-CoV-2 Omicron impacts infectivity and fusogenicity. Nature 603, 706-714.
Milan Bonotto, R., Boni, F., Milani, M., Chaves-Sanjuan, A., Franze, S., Selmin, F., Felicetti, T., Bolognesi, M., Konstantinidou, S., Poggianella, M., Marquez, C.L., Dattola, F., Zoppe, M., Manfroni, G., Mastrangelo, E., Marcello, A., 2022. Virucidal Activity of the Pyridobenzothiazolone Derivative HeE1-17Y against Enveloped RNA Viruses. Viruses 14.
Milani, M., Donalisio, M., Bonotto, R.M., Schneider, E., Arduino, I., Boni, F., Lembo, D., Marcello, A., Mastrangelo, E., 2021. Combined in silico and in vitro approaches identified the antipsychotic drug lurasidone and the antiviral drug elbasvir as SARS-CoV2 and HCoV-OC43 inhibitors. Antiviral Res 189, 105055.

Mirković, B., Markelc, B., Butinar, M., Mitrović, A., Sosič, I., Gobec, S., Vasiljeva, O., Turk, B., Čemažar, M., Serša, G., Kos, J., 2015. Nitroxoline impairs tumor progression in vitro and in vivo by regulating cathepsin B activity. Oncotarget 6, 19027-19042.
Mirković, B., Renko, M., Turk, S., Sosič, I., Jevnikar, Z., Obermajer, N., Turk, D., Gobec, S., Kos, J., 2011. Novel mechanism of cathepsin B inhibition by antibiotic nitroxoline and related compounds. ChemMedChem 6, 1351-1356.
Mitrović, A., Mirković, B., Sosič, I., Gobec, S., Kos, J., 2016. Inhibition of endopeptidase and exopeptidase activity of cathepsin B impairs extracellular matrix degradation and tumour invasion. Biological chemistry 397, 165-174.
Mitrović, A., Senjor, E., Jukić, M., Bolčina, L., Prunk, M., Proj, M., Nanut, M.P., Gobec, S., Kos, J., 2022. New inhibitors of cathepsin V impair tumor cell proliferation and elastin degradation and increase immune cell cytotoxicity. Computational and structural biotechnology journal 20, 4667-4687.
Mitrović, A., Sosič, I., Kos, Š., Tratar, U.L., Breznik, B., Kranjc, S., Mirković, B., Gobec, S., Lah, T., Serša, G., Kos, J., 2017. Addition of 2-(ethylamino)acetonitrile group to nitroxoline results in significantly improved anti-tumor activityin vitroandin vivo. Oncotarget 8, 59136-59147.
Mrhar, A., Kopitar, Z., Kozjek, F., Presl, V., Karba, R., 1979. Clinical pharmacokinetics of nitroxoline. Int J Clin Pharmacol Biopharm 17, 476-481.
Naber, K.G., Niggemann, H., Stein, G., Stein, G., 2014. Review of the literature and individual patients' data meta-analysis on efficacy and tolerance of nitroxoline in the treatment of uncomplicated urinary tract infections. BMC Infect Dis 14, 628.
Ou, T., Mou, H., Zhang, L., Ojha, A., Choe, H., Farzan, M., 2021. Hydroxychloroquine-mediated inhibition of SARS-CoV-2 entry is attenuated by TMPRSS2. PLOS Pathogens 17, e1009212-e1009212.
Ou, X., Liu, Y., Lei, X., Li, P., Mi, D., Ren, L., Guo, L., Guo, R., Chen, T., Hu, J., Xiang, Z., Mu, Z., Chen, X., Chen, J., Hu, K., Jin, Q., Wang, J., Qian, Z., 2020. Characterization of spike glycoprotein of SARS-CoV-2 on virus entry and its immune cross-reactivity with SARS-CoV. Nature Communications 11.
Padmanabhan, P., Desikan, R., Dixit, N.M., 2020. Targeting TMPRSS2 and Cathepsin B/L together may be synergistic against SARS-CoV-2 infection. PLOS Computational Biology 16, e1008461-e1008461.
Pišlar, A., Mitrovic, A., Sabotič, J., Fonovic, U.P., Nanut, M.P., Jakoš, T., Senjor, E., Kos, J., 2020. The role of cysteine peptidases in coronavirus cell entry and replication: The therapeutic potential of cathepsin inhibitors. PLoS Pathogens 16, 1-23.
Rajasekharan, S., Milan Bonotto, R., Nascimento Alves, L., Kazungu, Y., Poggianella, M., Martinez-Orellana, P., Skoko, N., Polez, S., Marcello, A., 2021. Inhibitors of Protein Glycosylation Are Active against the Coronavirus Severe Acute Respiratory Syndrome Coronavirus SARS-CoV-2. Viruses 13.
Regan, A.D., Shraybman, R., Cohen, R.D., Whittaker, G.R., 2008. Differential role for low pH and cathepsin-mediated cleavage of the viral spike protein during entry of serotype II feline coronaviruses. Veterinary microbiology 132, 235-248.
Saccon, E., Chen, X., Mikaeloff, F., Rodriguez, J.E., Szekely, L., Vinhas, B.S., Krishnan, S., Byrareddy, S.N., Frisan, T., Végvári, Á., Mirazimi, A., Neogi, U., Gupta, S., 2021. Cell-type-resolved quantitative proteomics map of interferon response against SARS-CoV-2. iScience 24, 102420-102420.
Schornberg, K., Matsuyama, S., Kabsch, K., Delos, S., Bouton, A., White, J., 2006. Role of Endosomal Cathepsins in Entry Mediated by the Ebola Virus Glycoprotein. Journal of Virology 80, 4174-4178.

Shang, J., Wan, Y., Luo, C., Ye, G., Geng, Q., Auerbach, A., Li, F., 2020. Cell entry mechanisms of SARS-CoV-2. Proceedings of the National Academy of Sciences 117, 11727-11734.
Shirato, K., Kawase, M., Matsuyama, S., 2013. Middle East respiratory syndrome coronavirus infection mediated by the transmembrane serine protease TMPRSS2. Journal of virology 87, 12552-12561.
Simmons, G., Gosalia, D.N., Rennekamp, A.J., Reeves, J.D., Diamond, S.L., Bates, P., 2005. Inhibitors of cathepsin L prevent severe acute respiratory syndrome coronavirus entry. Proceedings of the National Academy of Sciences of the United States of America 102, 11876-11881.
Simmons, G., Zmora, P., Gierer, S., Heurich, A., Pöhlmann, S., 2013. Proteolytic activation of the SARS-coronavirus spike protein: cutting enzymes at the cutting edge of antiviral research. Antiviral research 100, 605-614.
Sosič, I., Mirković, B., Arenz, K., Štefane, B., Kos, J., Gobec, S., 2013. Development of new cathepsin B inhibitors: Combining bioisosteric replacements and structure-based design to explore the structure-activity relationships of nitroxoline derivatives. Journal of Medicinal Chemistry 56, 521-533.
Sungnak, W., Huang, N., Becavin, C., Berg, M., Queen, R., Litvinukova, M., Talavera-Lopez, C., Maatz, H., Reichart, D., Sampaziotis, F., Worlock, K.B., Yoshida, M., Barnes, J.L., Network, H.C.A.L.B., 2020. SARS-CoV-2 entry factors are highly expressed in nasal epithelial cells together with innate immune genes. Nat Med 26, 681-687.
Turk, B., Turk, D., Turk, V., 2000. Lysosomal cysteine proteases: More than scavengers, pp. 98-111.
Wagenlehner, F.M., Munch, F., Pilatz, A., Barmann, B., Weidner, W., Wagenlehner, C.M., Straubinger, M., Blenk, H., Pfister, W., Kresken, M., Naber, K.G., 2014. Urinary concentrations and antibacterial activities of nitroxoline at 250 milligrams versus trimethoprim at 200 milligrams against uropathogens in healthy volunteers. Antimicrob Agents Chemother 58, 713-721.
WHO, 2021. https://covid19.who.int - WHO Coronavirus (COVID-19) Dashboard (accessed December 2021).
Wijma, R.A., Huttner, A., Koch, B.C.P., Mouton, J.W., Muller, A.E., 2018. Review of the pharmacokinetic properties of nitrofurantoin and nitroxoline. J Antimicrob Chemother 73, 2916-2926.
Willett, B.J., Grove, J., MacLean, O.A., Wilkie, C., De Lorenzo, G., Furnon, W., Cantoni, D., Scott, S., Logan, N., Ashraf, S., Manali, M., Szemiel, A., Cowton, V., Vink, E., Harvey, W.T., Davis, C., Asamaphan, P., Smollett, K.L., Tong, L., Orton, R.J., Hughes, J., Holland, P., Silva, V., Pascall, D.J., Puxty, K., da Silva Filipe, A., Yebra, G., Shaaban, S., Holden, M.T.G., Pinto, R.M., Gunson, R.N., Templeton, K.E., Murcia, P.R., Patel, A.A.H., Klenerman, P., Dunachie, S., Dunachie, S., Klenerman, P., Barnes, E., Brown, A., Adele, S., Kronsteiner, B., Murray, S.M., Abraham, P., Deeks, A., Ansari, M.A., de Silva, T.I., Turtle, L., Moore, S., Austin, J., Richter, A., Duncan, C., Payne, R., Ash, A., Koshy, C., Kele, B., Cutino-Moguel, T., Fairley, D.J., McKenna, J.P., Curran, T., Adams, H., Fraser, C., Bonsall, D., Fryer, H., Lythgoe, K., Thomson, L., Golubchik, T., Murray, A., Singleton, D., Beckwith, S.M., Mantzouratou, A., Barrow, M., Buchan, S.L., Reynolds, N., Warne, B., Maksimovic, J., Spellman, K., McCluggage, K., John, M., Beer, R., Afifi, S., Morgan, S., Mack, A., Marchbank, A., Price, A., Morriss, A., Bresner, C., Kitchen, C., Merrick, I., Southgate, J., Guest, M., Jones, O., Munn, R., Connor, T.R., Whalley, T., Workman, T., Fuller, W., Patel, A.A.H., Patel, B., Nebbia, G., Edgeworth, J., Snell, L.B., Batra, R., Charalampous, T., Beckett, A.H., Shelest, E., Robson, S.C., Underwood, A.P., Taylor, B.E.W., Yeats, C.A., Aanensen, D.M., Abudahab, K., Menegazzo, M., Joseph, A., Clark, G., Howson-Wells, H.C.,

Berry, L., Khakh, M., Lister, M.M., Boswell, T., Fleming, V.M., Holmes, C.W., McMurray, C.L., Shaw, J., Tang, J.W., Fallon, K., Odedra, M., Willford, N.J., Bird, P.W., Helmer, T., Williams, L.-A., Sheriff, N., Campbell, S., Raviprakash, V., Blakey, V., Moore, C.C., Sang, F., Debebe, J., Carlile, M., Loose, M.W., Holmes, N., Wright, V., Torok, M.E., Hamilton, W.L., Carabelli, A.M., Jermy, A., Blane, B., Churcher, C.M., Ludden, C., Aggarwal, D., Westwick, E., Brooks, E., McManus, G.M., Galai, K., Smith, K.S.K., Smith, K.S.K., Cox, M., Fragakis, M., Maxwell, P., Judges, S., Peacock, S.J., Feltwell, T., Kenyon, A., Eldirdiri, S., Davis, T., Taylor, J.F., Tan, N.K., Zarebski, A.E., Gutierrez, B., Raghwani, J., du Plessis, L., Kraemer, M.U.G., Pybus, O.G., Francois, S., Attwood, S.W., Vasylyeva, T.I., Jahun, A.S., Goodfellow, I.G., Georgana, I., Pinckert, M.L., Hosmillo, M., Izuagbe, R., Chaudhry, Y., Ryan, F., Lowe, H.H.L., Moses, S., Bedford, L., Cargill, J.S., Hughes, W., Moore, J., Stonehouse, S., Shah, D., Lee, J.C.D., Brown, J.R., Harris, K.A., Atkinson, L., Storey, N., Spyer, M.J., Flaviani, F., Alcolea-Medina, A., Sehmi, J., Ramble, J., Ohemeng-Kumi, N., Smith, P., Bertolusso, B., Thomas, C., Vernet, G., Lynch, J., Moore, N., Cortes, N., Williams, R.R.J., Kidd, S.P., Levett, L.J., Pusok, M., Grant, P.R., Kirk, S., Chatterton, W., Xu-McCrae, L., Smith, D.L., Young, G.R., Bashton, M., Kitchman, K., Gajee, K., Eastick, K., Lillie, P.J., Burns, P.J., Everson, W., Cox, A., Holmes, A.H., Bolt, F., Price, J.R., Pond, M., Randell, P.A., Madona, P., Mookerjee, S., Volz, E.M., Geidelberg, L., Ragonnet-Cronin, M., Boyd, O., Johnson, R., Pope, C.F., Witney, A.A., Monahan, I.M., Laing, K.G., Smollett, K.L., McNally, A., McMurray, C.L., Stockton, J., Quick, J., Loman, N.J., Poplawski, R., Nicholls, S., Rowe, W., Castigador, A., Macnaughton, E., Bouzidi, K.E., Sudhanva, M., Lampejo, T., Martinez Nunez, R.T., Breen, C., Sluga, G., Withell, K.T., Machin, N.W., George, R.P., Ahmad, S.S.Y., Pritchard, D.T., Binns, D., Wong, N., James, V., Williams, C.C.C.A.C., Illingworth, C.J., Jackson, C., de Angelis, D., Pascall, D.J., Mukaddas, A., Broos, A., da Silva Filipe, A., Mair, D., Robertson, D.L., Wright, D.W., Thomson, E.C., Starinskij, I., Tsatsani, I., Shepherd, J.G., Nichols, J., Hughes, J., Nomikou, K., Tong, L., Orton, R.J., Vattipally, S., Harvey, W.T., Sanderson, R., O'Brien, S., Rushton, S., Perkins, J., Blacow, R., Gunson, R.N., Gallagher, A., Wastnedge, E., Templeton, K.E., McHugh, M.P., Dewar, R., Cotton, S., Coupland, L., Stanley, R., Dervisevic, S., Spurgin, L.G., Smith, L., Graham, C., Padgett, D., Barton, E., Scott, G., Cross, A., Mirfenderesky, M., Swindells, E., Greenaway, J., Denton-Smith, R., Turnbull, R., Idle, G., Cole, K., Hollis, A., Nelson, A., McCann, C.M., Henderson, J.H., Crown, M.R., Yew, W.C., Stanley, W., Duckworth, N., Clarke, P., Walsh, S., Sloan, T.J., Bicknell, K., Impey, R., Wyllie, S., Elliott, S., Glaysher, S., Bradley, D.T., Killough, N.F., Wyatt, T., Bosworth, A., Vipond, B.B., Pearson, C., Allara, E., Robinson, E., Pymont, H.M., Osman, H., Muir, P., Hopes, R., Hutchings, S., Curran, M.D., Parmar, S., Thornton, A., Lackenby, A., Bishop, C., Bibby, D., Lee, D., Gallagher, E., Dabrera, G., Harrison, I., Hubb, J., Twohig, K.A., Chand, M., Ellaby, N., Manesis, N., Myers, R., Platt, S., Mbisa, T., Chalker, V., Yebra, G., Holden, M.T.G., Shaaban, S., Rooke, S., Birchley, A., Adams, A., Davies, A., Gaskin, A., Gatica-Wilcox, B., McKerr, C., Moore, C.C., Williams, C.C.C.A.C., Williams, C.C.C.A.C., Heyburn, D., De Lacy, E., Hilvers, E., Downing, F., Pugh, G., Jones, H., Asad, H., Coombes, J., Hey, J., Powell, J., Watkins, J., Evans, J.M., Fina, L., Gifford, L., Gilbert, L., Graham, L., Perry, M., Morgan, M., Bull, M., Pacchiarini, N., Craine, N., Corden, S., Kumziene-Summerhayes, S., Rey, S., Taylor, S., Cottrell, S., Jones, S., Edwards, S., Annett, T., Trotter, A.J., Mather, A.E., Aydin, A., Page, A.J., Baker, D.J., Foster-Nyarko, E., Kay, G.L., O'Grady, J., de Oliveira Martins, L., Meadows, L., Alikhan, N.-F., Prosolek, S.J., Rudder, S., Le-Viet, T., Casey, A., Ratcliffe, L., Singh, A., Mariappan, A., Baxter, C., Radulescu, C., Simpson, D.A., Lavin, D., Rogan, F., Miskelly, J., Fuchs, M., Tang, M., Carvalho, S.F., Bridgett, S., Skvortsov, T., Molnar, Z., Ramadan, N.A., Knight, B.A., Jones, C.R., Auckland, C., Morcrette, H., Poyner, J., Irish-Tavares, D., Witele, E., Hart, J., Mahungu, T.W., Haque, T., Bourgeois, Y., Fearn, C., Cook, K.F., Loveson, K.F., Goudarzi,

S., Evans, C., Partridge, D.G., Johnson, K., Yavus, M., Raza, M., Mower, C., Baker, P., Essex, S., Bonner, S., Murray, L.J., Watson, L.K., Liggett, S., Lawton, A.I., Lyons, R.A., Payne, B.A.I., Eltringham, G., Collins, J., Waugh, S., Burton-Fanning, S., Taha, Y., Jeanes, C., Gomes, A.N., Murray, D.R., Kimuli, M., Dobie, D., Ashfield, P., Best, A., Percival, B., Moles-Garcia, E., Ashford, F., Mirza, J., Crawford, L., Mayhew, M., Cumley, N., Megram, O., Frampton, D., Heaney, J., Byott, M., Houlihan, C., Williams, C.C.C.A.C., Nastouli, E., Lowe, H.H.L., Hartley, J.A., Breuer, J., Maftei, L., Ensell, L., Cotic, M., Mondani, M., Driscoll, M., Bayzid, N., Williams, R.R.J., Roy, S., Mahanama, A.I.K., Samaraweera, B., Wilson-Davies, E., Pelosi, E., Umpleby, H., Wheeler, H., Prieto, J.A., Saeed, K., Harvey, M., Jeremiah, S., Silviera, S., Aplin, S., Sass, T., Macklin, B., Crudgington, D., Sheridan, L.A., Cogger, B.J., Malone, C.S., Munemo, F., Huckson, H., Lewis, J., Easton, L.J., Mutingwende, M., Erkiert, M.J., Hassan-Ibrahim, M.O., Chaloner, N.J., Podplomyk, O., Randell, P.A., Nicodemi, R., Lowdon, S., Somassa, T., Richter, A., Beggs, A., Hesketh, A.R., Smith, C.P., Bucca, G., Ruis, C., Cormie, C., Higginson, E.E., Young, J., Dias, J., Kermack, L.M., Maes, M., Gupta, R.K., Forrest, S., Girgis, S.T., Davidson, R.K., O'Toole, Á., Rambaut, A., Jackson, B., Balcazar, C.E., Maloney, D., Scher, E., McCrone, J.T., Williamson, K.A., Gallagher, M.D., Medd, N., Colquhoun, R., Stanton, T.D., Williams, T., Hill, V., Jeffries, A.R., Temperton, B., Sambles, C.M., Studholme, D.J., Warwick-Dugdale, J., Jackson, L.M., Michelsen, M.L., Manley, R., Michell, S.L., Darby, A.C., Lucaci, A.O., Nelson, C., Wierzbicki, C., Vamos, E.E., Webster, H.J., Jackson, K.A., Rainbow, L., Hughes, M., Whitehead, M., Gemmell, M., Iturriza-Gomara, M., Eccles, R., Gregory, R., Haldenby, S.T., Paterson, S., Angyal, A., Keeley, A.J., Foulkes, B.H., Lindsey, B.B., Wang, D., Hornsby, H.R., Green, L.R., Pohare, M., Gallis, M., Parker, M.D., Whiteley, M., Smith, N., Wolverson, P., Zhang, P., Hansford, S.E., Hsu, S.N., Louka, S.F., de Silva, T.I., Freeman, T.M., Mori, M., Park, E.J., Hill, J.D., Dey, J., Ball, J., Chappell, J.G., McClure, P.C., Byaruhanga, T., Fanaie, A., Yaze, G., Hilson, R.A., Trebes, A., Green, A., Buck, D., MacIntyre-Cockett, G., Todd, J.A., Bassett, A.R., Whitwham, A., Langford, C.F., Rajan, D., Kwiatkowski, D., Harrison, E.M., Bronner, I.F., Tovar-Corona, J.M., Liddle, J., Durham, J., Bellis, K.L., Lewis, K., Aigrain, L., Redshaw, N.M., Davies, R.M., Moll, R.J., McCarthy, S.A., Lensing, S.V., Leonard, S., Farr, B.W., Scott, C., Beaver, C., Ariani, C.V., Weldon, D., Jackson, D.K., Betteridge, E., Tonkin-Hill, G., Johnston, I., Martincorena, I., Bonfield, J., Barrett, J.C., Sillitoe, J., Keatley, J.-P., Oliver, K., James, K., Shirley, L., Prestwood, L., Foulser, L., Gourtovaia, M., Dorman, M.J., Quail, M.A., Spencer Chapman, M.H., Park, N.R., Livett, R., Amato, R., Kay, S., Goodwin, S., Thurston, S.A.J., Rajatileka, S., Gonçalves, S., Lo, S., Sanderson, T., Maclean, A., Goldstein, E.J., Ferguson, L., Tomb, R., Catalan, J., Jones, N., Haughney, J., Robertson, D.L., Palmarini, M., Ray, S., Thomson, E.C., 2022. SARS-CoV-2 Omicron is an immune escape variant with an altered cell entry pathway. Nature Microbiology 7, 1161-1179.

Wu, M., Chen, Y., Xia, H., Wang, C., Tan, C.Y., Cai, X., Liu, Y., Ji, F., Xiong, P., Liu, R., Guan, Y., Duan, Y., Kuang, D., Xu, S., Cai, H., Xia, Q., Yang, D., Wang, M.W., Chiu, I.M., Cheng, C., Ahern, P.P., Liu, L., Wang, G., Surana, N.K., Xia, T., Kasper, D.L., 2020. Transcriptional and proteomic insights into the host response in fatal COVID-19 cases. Proc Natl Acad Sci U S A 117, 28336-28343.

Yadati, T., Houben, T., Bitorina, A., Shiri-Sverdlov, R., 2020. The Ins and Outs of Cathepsins: Physiological Function and Role in Disease Management. Cells 9, 1679-1679.

Zakaria, M.K., Carletti, T., Marcello, A., 2018. Cellular Targets for the Treatment of Flavivirus Infections. Front Cell Infect Microbiol 8, 398.

Zhao, H., Lu, L., Peng, Z., Chen, L.-L., Meng, X., Zhang, C., Ip, J.D., Chan, W.-M., Chu, A.W.-H., Chan, K.-H., Jin, D.-Y., Chen, H., Yuen, K.-Y., To, K.K.-W., 2022. SARS-CoV-2

Omicron variant shows less efficient replication and fusion activity when compared with Delta variant in TMPRSS2-expressed cells. Emerging Microbes & Infections 11, 277-283.
Zhao, M.M., Yang, W.L., Yang, F.Y., Zhang, L., Huang, W.J., Hou, W., Fan, C.F., Jin, R.H., Feng, Y.M., Wang, Y.C., Yang, J.K., 2021. Cathepsin L plays a key role in SARS-CoV-2 infection in humans and humanized mice and is a promising target for new drug development. Signal Transduct Target Ther 6, 134.
Zhou, N., Pan, T., Zhang, J., Li, Q., Zhang, X., Bai, C., Huang, F., Peng, T., Zhang, J., Liu, C., Tao, L., Zhang, H., 2016. Glycopeptide antibiotics potently inhibit cathepsin l in the late endosome/lysosome and block the entry of ebola virus, middle east respiratory syndrome coronavirus (MERS-CoV), and severe acute respiratory syndrome coronavirus (SARS-CoV). Journal of Biological Chemistry 291, 9218-9232.
Zhou, Y., Vedantham, P., Lu, K., Agudelo, J., Carrion, R., Nunneley, J.W., Barnard, D., Pöhlmann, S., McKerrow, J.H., Renslo, A.R., Simmons, G., 2015. Protease inhibitors targeting coronavirus and filovirus entry. Antiviral Research 116, 76-84.

Nitroxoline and its derivatives are effective cathepsin inhibitors of SARS-CoV-2 infection

*Rafaela Milan Bonotto[1], *Ana Mitrović[2,3], Izidor Sosič[3], Pamela Martinez-Orellana[1], Federica Dattola[1], Stanislav Gobec[3], Janko Kos[2,3] and Alessandro Marcello[1]

*Contributed equally to this work

[1]Laboratory of Molecular Virology, The International Centre for Genetic Engineering and Biotechnology (ICGEB), Padriciano, 99, 34149 Trieste, Italy.
[2]Department of Biotechnology, Jožef Stefan Institute, Jamova 39, 1000 Ljubljana, Slovenia
[3]Faculty of Pharmacy, University of Ljubljana, Aškerčeva cesta 7, 1000 Ljubljana, Slovenia

Highlights:

- Cathepsins are key host factors for SARS-CoV-2 entry.
- Cathepsin B inhibitors are active against SARS-CoV-2.
- Cathepsin activity is cell-type dependent.
- The antibiotic nitroxoline is a candidate for drug repurposing.

Declaration of interests

☒ The authors declare that they have no known competing financial interests or personal relationships that could have appeared to influence the work reported in this paper.

☐The authors declare the following financial interests/personal relationships which may be considered as potential competing interests:

The authors declare the international application number PCT/EP2021/083960 "8-hydroxyquinoline cysteine protease inhibitors for use in the prevention and/or treatment of a coronavirus disease". The authors declare that they have no known competing financial interests or personal relationships that could have appeared to influence the work reported in this paper.

On behalf of the authors:

Alessandro Marcello
Head, Laboratory of Molecular Virology
International Centre for Genetic Engineering and Biotechnology (ICGEB)
Padriciano, 99, 34149 Trieste, ITALY
http://www.icgeb.org/molecular-virology.html
Email: marcello@icgeb.org

Janko Kos
Faculty of Pharmacy
University of Ljubljana
Aškerčeva cesta 7, 1000 Ljubljana, Slovenia
Email: janko.kos@ffa.uni-lj.si
www.ffa.uni-lj.si